The Rise Times of Miniature Endplate Currents Suggest that Acetylcholine May Be Released Over a Period of Time

William Van der Kloot
Departments of Physiology and Biophysics and Pharmacological Sciences, Health Sciences Center, State University of New York, Stony Brook, New York 11794 USA

ABSTRACT Models of miniature endplate currents predict 20–80% rise times of 100 μs or less. These predictions are substantially less than most of the rise times recorded in the literature. New measurements were made of rise times at the frog neuromuscular junction using extracellular recording. The mean 20–80% rise time was 250 μs. Rise times were variable; at 20°C, 95% of them fell in a range from 140 to 460 μs. The most questionable assumption in the models is that the acetylcholine (ACh) is released instantaneously. Modifying the model, so that ACh diffuses from the vesicle through a pore, lengthens the rise time to observed levels. It has been proposed that ACh is released from the vesicle in exchange for Na^+. However, the rise times of miniature endplate currents recorded in solutions in which the Na^+ is replaced by sucrose are in the normal range. The Q_{10} for the rise of miniature endplate currents is ~2, which is consistent with the models and with temperature effects on pore formation in mast cells.

INTRODUCTION

My interest in miniature rise times was stimulated by a recent paper by Khanin et al. (1994). They were impressed by the evidence that the granules within mast cells release their contents through a pore that extends between the interior of the granule and the extracellular space (Almers et al., 1991; Monck and Fernandez, 1992; Spruce et al., 1990). Khanin et al. (1994) modeled acetylcholine (ACh) release from a synaptic vesicle in a motor nerve terminal, assuming that it occurred either through a fixed diameter pore or an expanding pore. They conclude that the ACh cannot be released by simply diffusing through a pore, as their modeling shows that ACh discharge would take more than 100 μs. They believe this too long to fit to the known time course of the rise of the miniature endplate current (MEPC). This idea sent me back to the literature to check on measured values of rise time. As will be seen shortly, it seems that the idea that rise times are less than 100 μs comes largely from models of MEPC generation, not from the observed values.

Modeling has played a significant role in the development of our understanding of the mechanism for the generation of MEPCs. MEPCs are generated by the release of a quantum of ACh that diffuses to the endplate and reacts with the ACh-gated endplate channels (AChR). The opening of the endplate channels allows Na^+ to flow inward to depolarize the endplate. The ACh is short-lived, because it is rapidly hydrolyzed by acetylcholinesterase (AChE) in the synaptic cleft. Magleby and Stevens (1972) proposed that the decay of the MEPC could be accounted for by the closing of the ACh-gated endplate channels (AChR). Further modeling incorporated the time courses of ACh diffusion in the synaptic cleft, the kinetics of ACh binding to and release from the AChR, the opening of the AChR channels, and the hydrolysis of ACh by the AChE in the cleft (Rosenberry, 1979; Wathey et al., 1979; Madsen et al., 1984; Nigmatullin et al., 1988; Parnas et al., 1990; Van der Kloot et al., 1994). In the most comprehensive model, the MEPC is built up from the Monte Carlo simulation of the movements of single ACh molecules (Salpeter, 1987; Bartol et al., 1991). These models are based on excellent measurements of the rate constants of the reactions and of the concentrations of AChR and AChE in the cleft and on the endplate (Salpeter, 1987). The models all assume that the ACh is released instantaneously. The rises predicted by the models are quite rapid, the 20–80% rise times are 100 μs or less (Table 1).

Most of the measurements show that the actual rise times of MEPCs are considerably longer than those predicted by the models (Table 2). Many of these values were obtained from voltage clamp recordings. According to Land et al. (1980), rise times measured from MEPCs recorded with the voltage clamp are prolonged unless rigorous precautions are taken to keep the electrode capacitance to ground low. Failure to observe this precaution might be responsible for the longer rise times reported by most observers who used the voltage clamp. Because of the instrumental noise added by the voltage clamp, many of the measurements of rise time were done on averaged MEPCs.

Some of these problems with the clamp can be avoided by recording the MEPCs with an external electrode, which records an extracellular voltage change generated by the current flow through the resistance of the extracellular pathway (Fatt and Katz, 1952; Gage, 1976). I will call such recordings externals. Externals should reliably measure the time courses of the MEPCs. Another advantage is that the

Received for publication 17 January 1995 and in final form 13 March 1995.

Address reprint requests to Dr. W. Van der Kloot, Department of Physiology and Biophysics, HSC, SUNY, Stony Brook, NY 11794–8661. Tel.: 516-444-3035; Fax: 516-444-3432; E-mail: wvanderkloot@sbccmail.bitnet.

0006-3495/95/07/148/07 $2.00

TABLE 1 Rise times from MEPC models

Time to peak (μs)	20–80% (μs)	Reference
207	65	Wathey et al., 1979
203	95	Madsen et al., 1984
320*	97 ± 8	Bartol et al., 1991
250*	100	Anglister et al., 1994

*Measured from illustrations in the publication.

instrumental noise on the externals is much lower than that contaminating voltage clamp records, so clean measurements can be made of the rise times. Most of the external measurements summarized in Table 2 also show that the rise times are substantially longer than those predicted by the models.

A potential problem with the extracellular measurements is that the pressure of the microelectrode against the nerve terminal narrows the cleft, which hinders ACh diffusion (Katz and Miledi, 1973). As microelectrode pressure also increases the amplitudes of the externals, probably many of the recordings were done with the electrode pushing on the tissue. Therefore I made some new measurements in which pressure was deliberately minimized. The measurements were made on frog endplates because most of the modeling has been based on their characteristics.

I also measured the rise time of MEPCs in a solution in which the Na^+ was replaced by sucrose. This was done because Khanin et al. (1994) proposed that ACh is exchanged for Na^+, which flows inward through the pore. They propose to present a hypothesis about how this exchange might speed the release of ACh through a pore.

MATERIALS AND METHODS

The frogs were *Rana pipiens*, obtained from a dealer and kept in the dark at 4°C. They were sacrificed by double-pithing. Ringer contained (in mM): NaCl, 120; KCl, 2.0; $CaCl_2$, 2.5; and *N*-Tris-(hydroxymethyl) methyl-2-aminoethanesulfonic acid/NaOH (TES) at pH 7.4, 4.0. Isotonic solution contained (in mM): sucrose, 240; KCl, 2.0; TES, 4.0. In many instances the Ringer contained 100 mM sucrose to increase miniature frequency when recording extracellular MEPCs (Fatt and Katz, 1952). Solution temperature was controlled with a Peltier plate.

Glass microelectodes filled with 3 M KCl were slurry-beveled to DC resistances of 1–2 MΩ for extracellular recording or 2–3.5 MΩ for intracellular recording (Lederer et al., 1979). Tip diameters were not measured, as presumably they were always <1 μm. The methods for voltage clamping, for recording the entire time course of the miniatures, and for A/D conversion have been described (Van der Kloot et al., 1994). The recording bandwidth was 0.1 Hz to 100 kHz for externals and 0.1 Hz to 4 kHz for clamped signals. Externals were recorded by first penetrating an endplate to make certain that miniature endplate potentials were present, then withdrawing the electrode and moving its tip until negative-going miniatures were observed. High gain was used so that very small miniatures could be detected, and then the electrode was moved to increase their amplitude. Care was taken to avoid pushing the electrode onto the tissue; once a good position was found for the electrode tip it was backed off slightly before recording was begun. The amplitudes of the observed externals ranged from 1 mV down to signals just above the noise, presumably because of the distance between the site of inward current flow and the electrode tip. Externals with amplitudes below an arbitrary threshold were not measured. The mean amplitude of the externals used for the rise measurements was 0.47 ± 0.094 mV (SEM) The frequency of measurable externals was usually <0.01 Hz.

TABLE 2 Measurements of miniature rise times

Animal	°C	To peak (μs)	20–80% (μs)	Reference
Voltage clamp measurements				
Toad	22.1	430*	120	Gage and McBurney, 1975
Human	23	400–700		Cull-Candy et al., 1979
Snake	20	300		Hartzell, 1975
Lizard	23	260	91	Land et al., 1980
Frog	20	255*	160	Madesen et al., 1987
Frog	9.5		500 ± 60	Dwyer, 1981
Mouse	30	640 ± 90	265 ± 30	Erxleben and Kriebel, 1988
External electrode measurements				
Toad	22	500*	100	Gage and McBurney, 1975
Frog‡	9.5		250 ± 30	Dwyer, 1981
Rat	37		167	Head, 1983
Rat (phasic)	20–22		180 ± 10§	Fedorov, 1987
Rat (tonic)	20–22		480 ± 80§	Fedorov, 1987
Mouse	24–26		780 ± 20§	Vautrin and Kriebel, 1992

*Estimated from record.
‡With Strickholm single electrode clamp.
§10–90% rise time.

Each miniature was digitized at 100 kHz and observed on the computer screen before the measurement was accepted. Miniatures were rejected when there was any suggestion that two signals were superimposed. The computer was programmed to identify and mark the peak of the miniature and then move point by point backward in time, marking the points where the signal first fell to <80% of the peak and <20% of the peak. Miniatures were averaged by aligning them at the midpoint of the rise (Land et al., 1980).

Confidence intervals for mean rise times were calculated by the bootstrap method, using 1000 estimates (Simon, 1992).

I used the MEPC model of Wathey et al. (1979). A quantum of ACh is released in the center of a circular endplate. As the ACh diffuses it reacts with the AChR to open endplate channels and is destroyed by AChE. The equations, parameters, and numerical methods used to solve the differential equations were presented recently (Van der Kloot et al., 1994) and therefore need not be reiterated here.

EXTERNALS

Fig. 1 shows a recording of an external and averaged externals at 5°C and 20°C. The rise times of externals recorded at 20°C and at 5°C are summarized in Table 3. The mean value at 20°C was 250 μs, which is almost identical to the values obtained on the frog by Dwyer (1981) with an extracellular voltage clamp but which is more than twice the duration predicted by the models.

Fig. 2 shows the distribution of the values in one long set of externals plotted on a probability axis. When plotted on a probability scale, points that fit a normal probability distribution function fall along a straight line (Sokal and Rohlf, 1981; Van der Kloot, 1989). The rise time points quite obviously do not fit to a line (Fig. 2 *A*). It is known that the duration of the rise is proportional to the amplitude

of the miniatures (Gage and McBurney, 1975). Miniature size measurements from an endplate do not fit well to a normal distribution, but log(miniature size) does (Van der Kloot, 1987, 1991). When the log(20–80%) rise time is plotted versus a probability scale, the points fall close to a line, except perhaps for the three or four largest (Fig. 2 *B*). It has been proposed that (miniature size)$^{2/3}$ may fit to a normal distribution, the logic being that vesicle size diameter is normally distributed and that miniature size might be proportional to vesicle volume (Van der Kloot, 1987, 1991; Bekkers et al., 1990). It is often difficult to determine whether log(miniature size) or (miniature size)$^{2/3}$ gives a better fit to a normal distribution. However, it is clear that (20–80% rise time)$^{2/3}$ plotted against probability does not fit a line as well as log(20–80% rise time) (compare Fig. 2, *B* and *C*). The spread of the rise times is notable; in the total of 1132 externals measured at 20°C, 95% of the rise times fell between 140 and 460 μs. As mentioned above, rise time is proportional to miniature size, so some of the spread is a result of variation in size. However, in the externals measured at 20°C the mean coefficient of variation of the amplitudes was 0.29 ± 0.03 (SEM), whereas that of the 20–80% rise times was 0.39 ± 0.053. This suggests that variables other than ACh content of the vesicles contributes to the rise time.

The Q_{10} for the rise of the externals in Table 3 is 1.9. This is larger than the 1.2 estimated by Gage and McBurney (1975) and somewhat lower than the 2.3 found by Dwyer (1981). For the rat, the Q_{10} is 1.6 (Fedorov, 1987) or 2.4 (Head, 1983). A Q_{10} of ~2 would seem a reasonable overall estimate. Cumulative plots of the distribution of the 20–80% rise times of externals at the two temperatures are shown in Fig. 3. The considerable dispersion of the points, mentioned above, is easily seen in the plot of those at 5°C.

Table 4 summarizes measurements of the rise times of MEPCs done with the voltage clamp at frog endplates soaked in isotonic sucrose solution. The measurements were done at 5°C, because at room temperature in this solution the membrane potentials soon are depolarized (Miledi et al., 1980). Endplates were usually held at positive potentials; the holding potential was determined by the ability of the clamp system to hold the membrane potential at the set level during the MEPCs. Most investigators have found that MEPC rise time is not altered by changes in membrane potential (reviewed by Gage, 1976). The MEPCs are outward currents, presumably carried by potassium ions flowing from the cell (Fig. 4). The mean amplitude of the MEPCs was only ~1 nA, which meant that individual signals were appreciably distorted by instrumental noise. From the 947 MEPCs measured, the mean 20–80% rise time was 410 μs. This may be somewhat shorter than the rise times in Ringer at 5°C (Table 3), but considering the noise on the MEPC signals I would hesitate to draw a firm conclusion on this point. It surely seems unlikely that Na^+ plays any substantial role in the release of ACh from the vesicles. Katz and Miledi (1969) also recorded miniature endplate potentials in isotonic $CaCl_2$ solution, which is further evidence that Na^+ does not play a special role in ACh release.

TABLE 3 Rise times of externally recorded MEPPs

	20–80% rise time (μs)	95% confidence interval	Number
20°C	380	330–420	83
	240	230–250	256
	250	210–290	46
	210	200–220	267
	270	250–300	71
	250	230–270	107
	220	200–220	302
	280	250–310	68
	230	190–250	36
	250	230–270	124
	240	230–250	251
	210	200–230	148
	240	220–250	251
	Mean = 250		Total = 2010
5°C	760	680–840	100
	630	730–900	100
	660	540–730	31
	630	520–710	29
	Mean = 670		Total = 260

MODELING MEPCs

The next question was how the predictions of the models are altered by changing temperature and when the ACh is not released instantaneously. Some of the predictions of the Wathey et al. (1979) model are shown in Fig. 5. To see how a decrease in temperature might alter the modeled MEPC, all of the rate constants for the reaction of ACh with AChE and AChR were divided by 3. And the diffusion coefficient for ACh was divided by 1.2. Fig. 5 *A* shows that this substantially decreases the peak number of channels opened. The 20–80% rise time is extended from 61 to 86

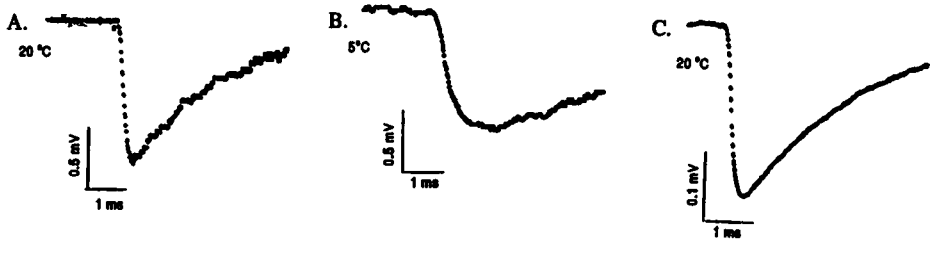

FIGURE 1 External recordings of miniatures. (A) Average of 301 externals recorded at 20°C. (*B*) Average of 100 externals recorded at 5°C. (*C*) A single external recorded at 20°C.

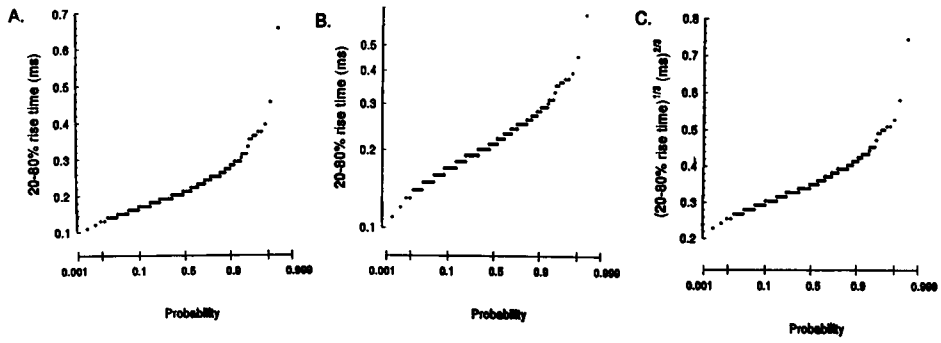

FIGURE 2 Probability plots of the 20–80% rise times of externals recorded at 20°C. (*A*) Plotting the rise times on an arithmatic scale. Note that the points would not fit well to a line ($R^2 = 0.82$). (*B*) Plotting logarithms of the rise time. Most of the points would fit fairly well to a line ($R^2 = 0.96$). (*C*) plotting the rise times to the 2/3 power ($R^2 = 0.88$). The fit to a line is not as good as when the logarithms are plotted.

μs, a factor of 1.4. The relatively small effect of temperature on rise time reflects the fact that the major determinant of rise time is the diffusion of ACh in the cleft.

The effects of ACh release over a period of time were assessed by adding to the model ACh release from the vesicle through a pore into the synaptic cleft. Fig. 5 *B* shows the modeled rise when the ACh released into the cleft, C_r, by time t (in seconds) was calculated by

$$C_r = C_0\left\{1 - \exp\left(\frac{-t}{VL/[\pi r_0^2 D]}\right)\right\},$$

where C_0 is the initial number of ACh molecules in the vesicle (10,000), V is the vesicle volume (2.65×10^{-17} cm^3), L is the pore length (1×10^{-6} cm), r_o is the radius of the pore (1×10^{-7} cm), and D is the diffusion coefficient for ACh through the pore (4×10^{-6} cm^2 s^{-1}) (Almers et al., 1991; Khanin et al., 1994). When the ACh is released by diffusing through this pore, the predicted 20–80% rise time is 185 μs, much closer to measured values. There is also a slowing of the decay of the MEPC (Fig. 5 *C*). This lengthening of the decay also makes the model more like the data, as a number of investigators have found that the decay of the MEPC is slower than that predicted from the open times of the endplate channels estimated by fluctuation analysis (Colquhoun et al., 1977; Gage and Van Helden, 1979; Katz and Miledi, 1973; Cull-Candy et al., 1979; Van der Kloot et al., 1994).

The number of channels opening per time interval is shown in Fig. 5 *D*. These calculations were made so that the estimates of the times of channel opening in the model can be compared with those obtained by the deconvolution of MEPCs (Cohen et al., 1981; Van der Kloot et al., 1994). When release is through the pore, the peak number of channels opening in any time bin is decreased and the time over which channels are opening is extended. This picture resembles the time course of channel opening calculated from MEPCs (Van der Kloot et al., 1994).

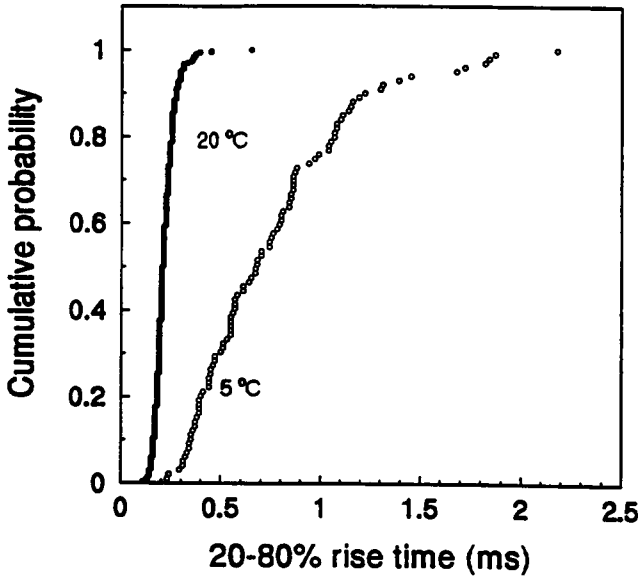

FIGURE 3 Cumulative plots of the 20–80% rise times of externals recorded from an endplate at 20°C and from one at 5°C. The mean at 20°C is 210 μs ($n = 301$); at 5°C the mean is 760 μs ($n = 100$).

DISCUSSION AND SUMMARY

Most of the values for the rise time of the MEPC in the literature are more than twice the values predicted by models of MEPC generation. The models are based on extensive measurements of the kinetics of ACh interaction with the AChR and with AChE, along with careful measurements of the density of the AChR and the AChE at the frog neuromuscular junction. In the lizard, reducing the AChR to 38% of normal lengthens the 20–80% rise time by a factor of 2.1 (Land et al., 1980), which shows that large errors in the measurements would be required to bring the models and the measurements into line. The modelers have been aware of the problem of the fast rise time and usually use a diffusion coefficient for ACh in the cleft that is one-third to one-fourth of its value in free solution. I used the same low diffusion coefficent in the modeling. In the Wathey et al. (1979) model, raising the diffusion coefficient threefold, to 9×10^{-6} cm^2 s^{-1}, reduces the 20–80% rise time to 34.1 μs. Land et al. (1980) estimated the diffusion coefficient from the rising phase of MEPCs as 4×10^{-6} cm^2 s^{-1}, but this estimate is based on the shortest estimates of rise time in the literature and on the assumption that ACh release from the vesicle is instantaneous.

Instantaneous release seems to be the most questionable assumption in the models. Even if the contents of the vesicle are ejected abruptly into the synaptic cleft by

TABLE 4 Rise times of MEPCs at 5°C in isotonic sucrose solution

Holding potential (mV)	20–80% rise time (μs)	95% confidence interval (μs)	Number
+20	410	340–460	54
−24	720	630–790	50
+50	440	390–470	100
+64	430	380–480	50
+60	400	350–440	99
+42	470	420–510	101
+70	450	410–470	200
+63	370	330–400	92
+100	390	360–410	201

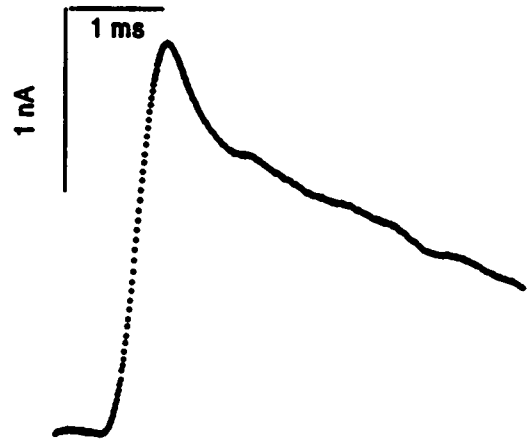

FIGURE 4 The average of 199 MEPCs recorded at a holding potential of +100 mV in a preparation in isotonic sucrose solution at 5°C.

exocytosis, some time might be required for the dissociation of the ACh from anionic binding sites (Nanavati and Fernandez, 1993). Fig. 3 *B* shows that when the model includes release by diffusion through a pore between the vesicle and the synaptic cleft the rise time lengthens toward measured values. In this calculation the diffusion coefficient for ACh in the pore was assumed to be the same as in the cleft. Reducing the diffusion coefficient in the pore to one-fourth of its value in the cleft, which Khanin et al. (1994) estimate to be the maximal effect of hindered diffusion in the pore, increases the 20–80% rise time to 425 μs. This is longer than the measured values in the frog. However, the merits of this line of speculation are uncertain, as the value chosen for the diffusion coefficient in the cleft is already well below that in free solution. The most defensible conclusions are that the rise of the MEPC is slower than predicted by the models and that the most likely deficiency in the models is the assumption that the ACh is released from the vesicle instantaneously.

Another problem that modelers have yet to tackle is the spread of the values of the measured rise times. The shortest are less than one-fourth of the length of the longest. Gage and McBurney (1975) proposed that there are two distinct populations of MEPCs, with rapid and slow rise times. Distributions like those in Fig. 2 *B* suggest that most of the rise times could be fit by a single log-normal distribution, with the possible exception of the two longest data points. Some of the spread is a result of variation in the amount of ACh per quantum, as the rise time is correlated with amplitude, but in many data sets the coefficient of variation of the rise times is twice that of the amplitudes. One possible explanation is that some of the spread is caused by variations in the rate of release of ACh from the vesicles.

The Q_{10} for the rise times appears to be ~2. Khanin et al. (1994) make a point of the temperature coefficient, stating that this is evidence that diffusion cannot account for the release of ACh from the vesicle. To support this idea, they cite the Q_{10} of 3–4 measured for the synaptic delay, i.e., the interval between the peak of the nerve terminal action potential and the beginning of the endplate depolarization (Katz and Miledi, 1964; Barrett and Stevens, 1972; Dudel, 1984; Parnas et al., 1989; Van der Kloot and Molgó, 1994). The synaptic delay includes the time required for the exocytotic apparatus to be activated by inflowing Ca^{2+} and to open the vesicle to the synaptic cleft so that ACh is released to open endplate channels. This is a complex process involving a battery of specialized proteins (reviewed by Van der Kloot and Molgó, 1994). What the temperature sensitivity of this sequence of events has to do with the rise time, which begins when the first ACh molecules reach the endplate, is not clear to me.

The effects of temperature on pore formation in mast cells seem to fit well with measurements of ACh release at the neuromuscular junction. The temperature dependence of the opening and closing of pores between the secretory granule of mouse mast cells and the extracellular space show that the opening has a high activation energy, 23 kcal/mol (Oberhauser et al., 1992). The Q_{10} (at 10°C) for the mean interval between irreversible fusion events is 4.1. Recall that the Q_{10} for the synaptic delay at the neuromuscular junction is 3–4 and that synaptic delay includes the time required for the vesicle to open. As the Q_{10} for irreversible fusion is high, it is reasonable that the Q_{10} for the synaptic delay is high also. On the other hand, closure of the fusion pore in the mast cell has a weak temperature dependence above 13°C; below 13°C it is temperature independent. The most comparable information we have at the neuromuscular junction is that the amount of ACh released per quantum appears to be independent of the temperature (Cohen and Van der Kloot, 1983; Van der Kloot and Cohen, 1984). This suggests that the vesicles release all of the ACh they contain. There is no indication that the amount of ACh released depends on how long a pore remains open.

The major point is that current models of MEPC generation do not account adequately for measured values of the rise time, probably because the release of the ACh from the vesicle is not instantaneous. The decay of the MEPC often cannot be accounted for simply by the closing of the endplate channels, because the decay of the MEPC is slower than predicted from the kinetics of channel closing (Colquhoun et al., 1977; Gage and Van Helden, 1979; Katz

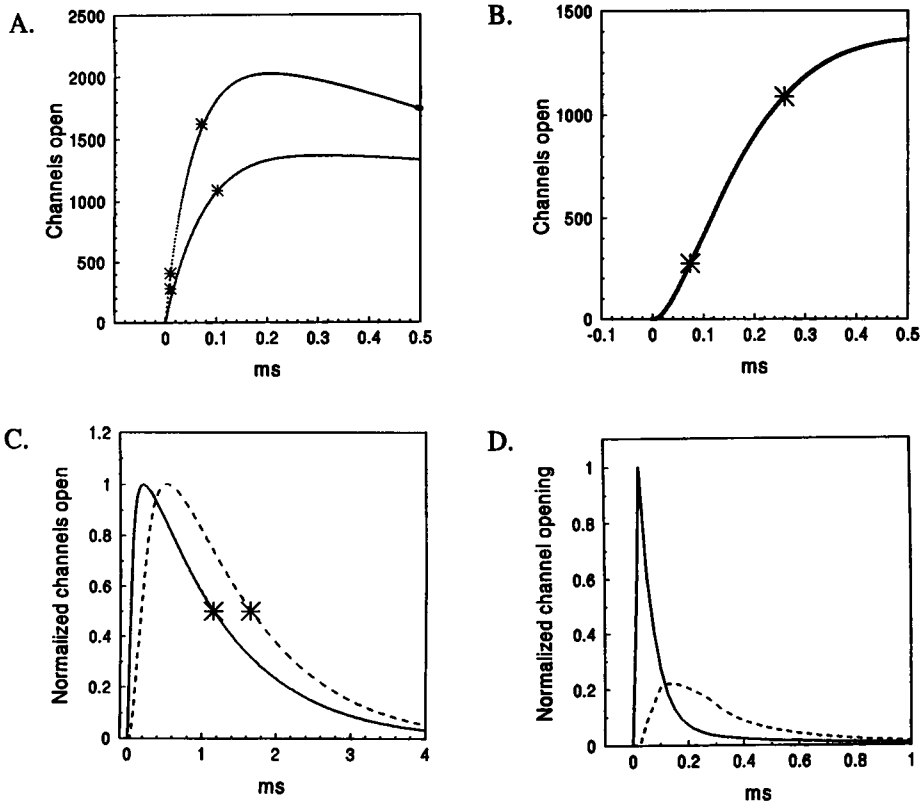

FIGURE 5 Results of calculations with the model of MEPC generation of Wathey et al. (1979). (*A*) Effects of lowering the temperature (*dotted line*, room temperature; *solid line*, lower temperature). The stars indicate the 20 and 80% points on the rise. At room temperature the 20–80% rise time is 61 μs; at the lower temperature it is 87 μs. (*B*) The rise in a model in which the ACh is not released instantaneously but diffuses from the vesicle through a pore. The stars indicate the 20 and 80% points; the 20–80% rise time is 185 μs. (*C*) The MEPCs generated by the normal model (*solid line*) and when the ACh diffuses from the vesicle through a pore (*dashed line*). The stars indicate the points where the number of open channels is 50% of that at the peak. The 50% decay time when the ACh is released instantaneously is 1.15 ms; when the ACh is released through a pore it is 1.65 ms. (*D*) The same models shown in *C* but showing the number of channels opening per time interval. The plots are normalized so that the total number of channels opened is the same. The normal model opens 3097 channels, whereas the pore model opens 2124 channels.

and Miledi, 1973; Cull-Candy et al., 1979; Van der Kloot et al., 1994). There appears to be a tail of ACh release into the synaptic cleft. The effects of this extended release are striking when the AChE is inhibited (Van der Kloot et al., 1994; Naves and Van der Kloot, in preparation). We do not yet fully understand how transmitter is released at this synapse.

I am grateful to Ira S. Cohen for discussions and to Judy Samarel for assistance with the preparation of the manuscript.
This work was supported by grant 10320 from the National Institute of Neurological and Communicative Disorders and Stroke.

REFERENCES

Almers, W., L. J. Breckenridge., A. Iwata., A. K. Lee., A. E. Spruce., and F. W. Tse. 1991. Millisecond studies of single membrane fusion events. *Ann. NY Acad. Sci.* 636:318–327.

Anglister, L., J. R. Stiles., and M. M. Salpeter. 1994. Acetylcholinesterase density and turnover number at frog neuromuscular junctions, with modeling of their role in synaptic function. *Neuron.* 12:783–794.

Barrett, E. E., and C. F. Stevens. 1972. Quantal independence and uniformity of presynaptic release kinetics at the frog neuromuscular junction. *J. Physiol. (Lond.).* 227:665–698.

Bartol, T. M. Jr., B. R. Land, E. E. Salpeter, and M. M. Salpeter. 1991. Monte Carlo simulation of miniature endplate current generation in the vertebrate neuromuscular junction. *Biophys. J.* 59:1290–1307.

Bekkers, J. M., G. B. Richerson, and C. F. Stevens. 1990. Origin of variability in quantal size in cultured hippocampal neurons and hippocampal slices. *Proc. Natl. Acad. Sci. USA.* 87:5359–5362.

Cohen, I., W. Van der Kloot, and D. Attwell. 1981. The timing of channel opening during miniature end-plate currents. *Brain Res.* 223:185–189.

Cohen, I. S., and W. Van der Kloot. 1983. Effects of low temperature and terminal membrane potential on quantal size at frog neuromuscular junction. *J. Physiol. (Lond.).* 336:335–344.

Colquhoun, D., W. A. Large, and H. P. Rang. 1977. An analysis of the action of a false transmitter at the neuromuscular junction. *J. Physiol. (Lond.).* 266:361–395.

Cull-Candy, S. G., R. Miledi, and A. Trautmann. 1979. End-plate currents and acetylcholine noise at normal and myasthenic human end-plates. *J. Physiol. (Lond.).* 287:247–265.

Dudel, J. 1984. Control of quantal transmitter release at frog's nerve terminals. II. Modulation by de- or hyperpolarizing pulses. *Pflugers Arch. Eur. J. Physiol.* 402:235–243.

Dwyer, T. M. 1981. The rising phase of the miniature endplate current at the frog neuromuscular junction. *Biochim. Biophys. Acta.* 646:51–60.

Fatt, P., and B. Katz. 1952. Spontaneous subthreshold activity at motor nerve endings. *J. Physiol. (Lond.).* 117:109–128.

Fedorov, V. V. 1987. Postsynaptic currents in phasic and tonic muscle fibers of the rat. *Neirophiziologiya.* 19:120–129.

Gage, P. W. 1976. Generation of end-plate potentials. *Physiol. Rev.* 56: 177–247.

Gage, P. W., and R. N. McBurney. 1975. Effects of membrane potential, temperature and neostigmine on the conductance change caused by a quantum of acetylcholine at the toad neuromuscular junction. *J. Physiol. (Lond.).* 244:385–407.

Gage, P. W., and D. Van Helden. 1979. Effects of permeant monovalent cations on end-plate channels. *J. Physiol. (Lond.).* 288:509–528.

Head, S. D. 1983. Temperature and end-plate currents in rat diaphragm. *J. Physiol. (Lond.).* 334:441–459.

Katz, B., and R. Miledi. 1964. The measurement of synaptic delay, and the time course of acetylcholine release at the neuromuscular junction. *Proc. R. Soc. Lond. Ser. B Biol. Sci.* 161:483–495.

Katz, B., and R. Miledi. 1969. Spontaneous and evoked activity of motor nerve endings in calcium Ringer. *J. Physiol. (Lond.).* 203:689–706.

Katz, B., and R. Miledi. 1973. The binding of acetylcholine to receptors and its removal from the synaptic cleft. *J. Physiol. (Lond.).* 231: 549–574.

Khanin, R., H. Parnas, and L. Segel. 1994. Diffusion cannot govern the discharge of neurotransmitter in fast synapses. *Biophys. J.* 67(3): 966–972.

Land, B. R., E. E. Salpeter, and M. M. Salpeter. 1980. Acetylcholine receptor site density affects the rising phase of miniature endplate currents. *Proc. Natl. Acad. Sci. USA.* 77:3736–3740.

Lederer, W. J., A. J. Spindler, and D. A. Eisner. 1979. Thick slurry beveling: a new technique for bevelling extremely fine microelectrodes and micropipettes. *Pflugers Arch. Eur. J. Physiol.* 381:287–288.

Madsen, B. W., R. O. Edeson, H. S. Lam, and R. K. Milne. 1984. Numerical simulation of miniature endplate currents. *Neurosci. Lett.* 48:67–74.

Magleby, K. L., and C. F. Stevens. 1972. A quantitative description of end-plate currents. *J. Physiol. (Lond.).* 223:173–197.

Miledi, R., S. Makajima, and I. Parker. 1980. Endplate currents in sucrose solution. *Proc. R. Soc. Lond. Ser. B Biol. Sci.* 211:135–141.

Monck, J. R., and J. M. Fernandez. 1992. The exocytotic fusion pore. *J. Cell. Biol.* 119:1395–1404.

Nanavati, C., and J. M. Fernandez. 1993. The secretory granule matrix: a fast-acting smart polymer. *Science.* 259:963–965.

Nigmatullin, N. R., V. A. Snetkov, E. E. Nikolskii, and L. G. Magazanik. 1988. Modelling of miniature endplate current. *Neirofiziologiya.* 20: 390–397.

Oberhauser, A. F., J. R. Monck, and J. M. Fernandez. 1992. Events leading to the opening and closing of the exocytotic fusion pore have markedly different temperature dependencies: kinetic analysis of single fusion events in patch-clamped mouse mast cells. *Biophys. J.* 61:800–809.

Parnas, H., M. Flashner, and M. E. Spira. 1989. Sequential model to describe the nicotinic synaptic current. *Biophys. J.* 55:875–884.

Parnas, H., I. Parnas, and L. A. Segel. 1990. On the contribution of mathematical models to the understanding of neurotransmitter release. *Int. Rev. Neurobiol.* 32:1–50.

Rosenberry, T. L. 1979. Quantitative simulation of endplate currents at neuromuscular junctions based on the reaction of acetylcholine with acetycholine receptor and acetylcholinesterase. *Biophys. J.* 26:263–290.

Salpeter, M. M. 1987. Vertebrate neuromuscular junctions: general morphology, molecular organization, and functional consequences. *In* The Vertebrate Neuromuscular Junction. M. M. Salpeter, editor. Alan R. Liss, New York. 1–54.

Simon, J. L. 1992. Resampling: The New Statistics. Resampling Stats, Inc., Arlington, VA.

Sokal, R. R., and F. J. Rohlf. 1981. Biometry. W. H. Freeman, New York.

Spruce, A. E., L. J. Breckenridge, A. K. Lee, and W. Almers. 1990. Properties of the fusion pore that forms during exocytosis of a mast cell secretory vesicle. *Neuron.* 4:643–654.

Van der Kloot, W. 1987. Pretreatment with hypertonic solutions increases quantal size at the frog neuromuscular junction. *J. Neurophysiol.* 57: 1536–1554.

Van der Kloot, W. 1989. Statistical and graphical methods for testing the hypothesis that quanta are made up of subunits. *J. Neurosci. Methods.* 27:81–89.

Van der Kloot, W. 1991. The regulation of quantal size. *Prog. Neurobiol.* 36:93–130.

Van der Kloot, W., O. P. Balezina, J. Molgó, and L. A. Naves. 1994. The timing of channel opening during miniature endplate currents at the frog and mouse neuromuscular junctions: effects of fasciculin-2, other anticholinesterases and vesamicol. *Pflugers Arch. Eur. J. Physiol.* 428: 114–126.

Van der Kloot, W., and I. S. Cohen. 1984. Temperature effects on spontaneous and evoked quantal size at the frog neuromuscular junction. *J. Neurosci.* 4:2200–2203.

Van der Kloot, W., and J. Molgó. 1994. Quantal acetylcholine release at the vertebrate neuromuscular junction. *Physiol. Rev.* 74:899–991.

Wathey, J. C., M. M. Nass, and H. A. Lester. 1979. Numerical reconstruction of the quantal event at nicotinic synapses. *Biophys. J.* 27:145–164.